Investigation on microstructure and electrical properties of CuAl$_{1-x}$Y$_x$O$_2$ ceramics by electrical impedance spectroscopy

CrossMark

Ying Wang [a], Lei Cheng [b], Mankang Zhu [a, *], Jun Zhao [b], Yudong Hou [a]

[a] College of Materials Science and Engineering, Beijing University of Technology, Beijing 100124, China
[b] Tianjin Aviation Electro-Mechanical Co. Ltd., Tianjin 300308, China

ARTICLE INFO

ABSTRACT

Y$_2$O$_3$-doped CuAlO$_2$ (CAO) ceramics with delafossite structure were prepared by the solid state oxide reaction method. X-ray diffraction analysis demonstrates that the most of the Y^{3+} enter into the CAO lattice to occupy Al^{3+} sites, while the second phase Al$_5$Y$_3$O$_{12}$ is formed due to the limited solubility of Y$_2$O$_3$ into CAO. The activation energies derived from the temperature depending on bulk conductivity and dielectrically relaxation present a tend to decrease similarly as the Y$_2$O$_3$ is added. Besides, the carrier mobility rises gradually as Y$_2$O$_3$ is added, and turns to sharp augment at the Y$_2$O$_3$ addition reaching to $x = 0.04$. Hence, at small Y$_2$O$_3$ addition, the emergence of the insulated Al$_5$Y$_3$O$_{12}$ limits the conductivity; on the other hand, the sharp augment of carrier mobility results from the increase of the conductivity when Y$_2$O$_3$ addition is over $x = 0.04$.

1. Introduction

Transparent conducting oxides (TCOs) is of great interest because of the wide range of applications such as flat panel displays, organic light emitting diodes, thin film transistors, touch panels and optical waveguides, etc. [1]. However, the development of transparent devices basically requiring *p-n* junctions was hampered due to the lack of *p*-type transparent semiconductors with good performance. The situation didn't change until Kawazoe et al. [2] successfully fabricated *p*-type CuAlO$_2$ (CAO) thin film in 1997. Since then, CAO has attracted a great interest for its application ranging from *p-n* junction to transistors.

Unfortunately, the conductivity of CAO is 2–3 orders of magnitude lower than that of commonly *n*-type TCOs like indium-tin oxide [2,3]. Consequently, it is a very necessary and exigent task to improve the electrical conductivity of CAO. As it is well known, the electrical conductivity of a semiconductor is proportional to the concentration and mobility of its carriers [4,5]. Doping CAO with acceptors is adopted as one of the most effective ways to increase the carrier density and consequently improve the electrical conductivity [6–9]. It is believed that the acceptor doping can increase the electrical conductivity of p-type semiconductor by contributing

to the hole concentration, and thus decrease the optical transmittance because more carriers could absorb more photons [8–11].

CAO is a *p*-type semiconductor with delafossite structure. For CuMO$_2$, the increase of the size of M^{3+} cation decreases distance of Cu–O and increases the Cu–Cu distance [12], which brings in the lattice distortion and the variation of the carrier mobility [13]. Jiang et al. reported that Cr doping into CAO can modify the structure of the top of valence band (VB) because Cr 3d state contributes to VB [14]. However, the coexistence of Cr^{2+} and Cr^{3+} will increase the carrier density and decrease the optical transmission. Therefore, in CAO-based solid solutions, the isovalent substitution for Al^{3+} in delafossite CAO will provide a routine to realize the variation in carrier mobility while keep the optical behaviors.

In the work, trivalent Y^{3+} is applied to occupy the Al^{3+} site of the delafossite CAO. The effect of Y$_2$O$_3$ addition on the structure and electrical properties of CAO ceramics will be investigated. By means of the electrical impedance spectroscopy (EIS), the electrical conductance and dielectric relaxation behavior are analyzed. Combined with the carrier mobility, the relation between electrical properties and microstructure is probed.

2. Experimental details

CuAl$_{1-x}$Y$_x$O$_2$ ($x = 0$–0.06) samples were produced by solid oxide reaction method using Cu$_2$O, Al(OH)$_3$ and Y$_2$O$_3$ (purity higher than 99%) powders as raw materials. The powders were weighed

* Corresponding author.
    E-mail address: zhumk@bjut.edu.cn (M. Zhu).

according to stoichiometric ratio and mixed through ball milling, with partially stabilized zirconia balls as media, in alcohol for 12 h. After drying, the mixture was calcined in a covered alumina crucible at 1100 °C for 10 h. The calcined powders were remilled for 12 h, and then pressed into disks of 11.5 mm in diameter at around 100 MPa using polyvinyl alcohol as binder. The green disks were debinded at 560 °C for 6 h, and then sintered at 1200 °C for 4 h in a sealed alumina crucible. After polishing, the sample for the impedance measurement was sputtered with Au electrodes on both sides while the sample for Hall measurement was sputtered with Au electrodes through a mask. The mask consists of four round pores with a diameter of 1.0 mm arranging in a rectangle form. The samples as-sputtered with Au electrodes were annealed at 450 °C for 30 min in air.

The crystal structure was examined by an x-ray diffractometer (XRD, Bruker D8 Advance, Germany) in the θ- 2θ configuration using Cu Kα radiation. The electrical impedance response was recorded by an impedance analyzer (Concept 400, Novocontrol Technologies, Germany) in a frequency range between 1 Hz and 10 MHz and temperature range between −150 °C and −75 °C. Hall measurements were carried out at room temperature using the van der Pauw method by a Hall System (HL5550 LN2 CRYOSTAT, Nano metrics).

3. Results and discussion

3.1. Structural properties

All the samples show a high relative density above 95% bases on the Archimedes method, indicating their good sintering behavior. Besides, Fig. 1 shows XRD patterns of the $CuAl_{1-x}Y_xO_2$ samples with different x values. When $x = 0$, all diffractions could be assigned to delafossite CAO (JCPDS 76-2398, $R\bar{3}m$). With increasing Y_2O_3 content in CAO, there appear new diffractions located at 29.8°, 33.4° and 35.0°, matching to those of cubic $Al_5Y_3O_{12}$ (JCPDS 73-1370). To find out the solubility of Y_2O_3 into CAO lattice, fining XRD patterns were recorded as shown in Fig. 2. As seen in Fig. 2, both the (101) diffraction around 36.68° and (012) diffraction around 37.85° shift toward lower angles with the increasing Y_2O_3 content, illustrating that the Y^{3+} doping leads to lattice expansion. The lattice expansion implies that Y^{3+} enters into the CAO structure to occupy the Al^{3+} sites because of the larger radius of Y^{3+} (0.892 Å) than that of Al^{3+}
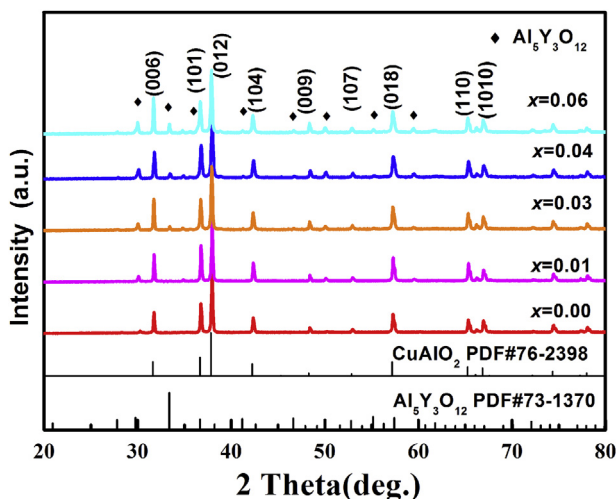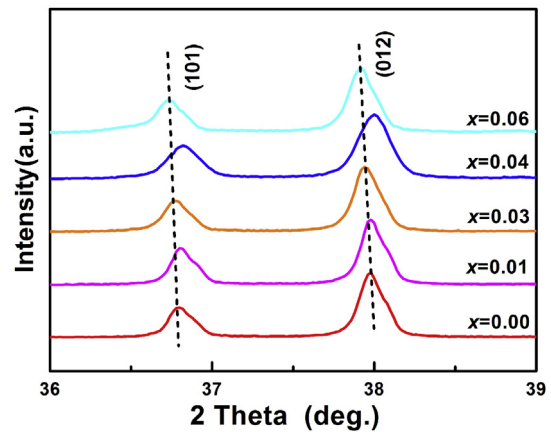

Fig. 2. Fining–scanning XRD patterns of the $CuAl_{1-x}Y_xO_2$ samples in 2θ range from 36° to 39°. The oblique dashed lines illustrate the shift of (1 0 1) and (0 1 2) peaks.

(0.530 Å). Besides, the gradual shift to small angle of the (101) and (012) diffractions demonstrates the increasing of the amount of Y^{3+} entering into the CAO lattice. However, accompanied by the increasing of the amount of Y^{3+} entering into CAO lattice, the intensity of the diffractions assigned to $Al_5Y_3O_{12}$ goes up with the increasing Y_2O_3 content. Hence, the appearance of the second phase $Al_5Y_3O_{12}$ is thought to be resulted from the difference of reaction activity among the raw materials, including $Al(OH)_3$, Y_2O_3 and Cu_2O, respectively.

3.2. Impedance analysis

EIS is the most reliable and important technique to study the electrical and dielectric properties and process of a material, and has been used to study many kinds of materials in previous works [15–17]. In our work, the impedance spectra of CAO with different Y_2O_3 doping are adopted to observe the effect of the Y_2O_3 content on the electrical properties of CAO ceramics.

The complex impedance (Nyquist) plots of CAO ceramics measured at temperatures from −125 °C to −75 °C are shown in Fig. 3. In the measuring temperature range, the Nyquist plots of the CAO present deformed semicircular arcs, which suggest that the relaxation in CAO is not an ideal Debye relaxation [18,19]. And with the temperature increase, the arcs become depressed, which
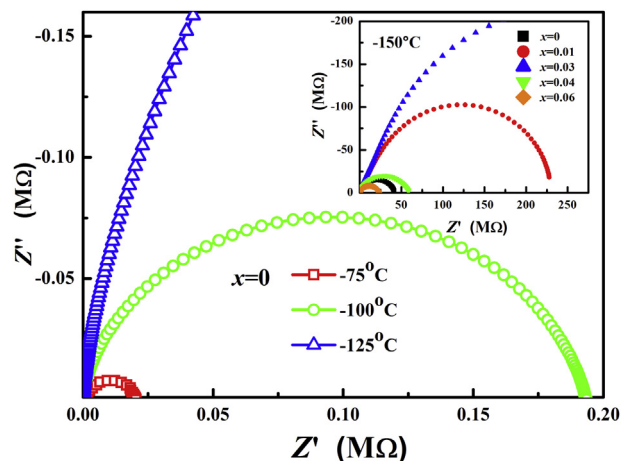

Fig. 1. XRD patterns of the $CuAl_{1-x}Y_xO_2$ ceramics. The symbol ◆ demonstrates the impurity phase $Al_5Y_3O_{12}$.

Fig. 3. Complex impedance plots for the $CuAlO_2$ ceramic at different temperatures. Inset gives complex impedance plots for the $CuAl_{1-x}Y_xO_2$ ceramics at −150 °C.